ADVANCED FUNCTIONAL MATERIALS

DOI: 10.1002/adfm.200800541

Towards Self-Powered Nanosystems: From Nanogenerators to Nanopiezotronics**

By *Zhong Lin Wang**

Developing wireless nanodevices and nanosystems are of critical importance for sensing, medical science, defense technology, and even personal electronics. It is highly desirable for wireless devices and even required for implanted biomedical devices that they be self-powered without use of a battery. It is essential to explore innovative nanotechnologies for converting mechanical energy (such as body movement, muscle stretching), vibrational energy (such as acoustic or ultrasonic waves), and hydraulic energy (such as body fluid flow) into electrical energy, which will be used to power nanodevices without a battery. This is a key step towards self-powered nanosystems. We have demonstrated an innovative approach for converting mechanical energy into electrical energy by piezoelectric zinc oxide nanowire (NW) arrays. The operation mechanism of the electric generator relies on the unique coupling of the piezoelectric and semiconducting properties of ZnO as well as the gating effect of the Schottky barrier formed between the metal tip and the NW. Based on this mechanism, we have recently developed a DC nanogenerator (NG) driven by the ultrasonic wave in a biofluid and a textile-fiber-based NG for harvesting low-frequency mechanical energy. Furthermore, a new field, ''nanopiezotronics'', has been developed, which uses coupled piezoelectric–semiconducting properties for fabricating novel and unique electronic devices and components. This Feature Article gives a systematic description of the fundamental mechanism of the NG, its rationally innovative design for high output power, and the new electronics that can be built based on a piezoelectric-driven semiconducting process. A perspective will be given about the future impact of the technologies.

1. From Nanodevices to Nanosystems and to Self-Powered Nanosystems

With the threat of global warming and energy crises, searching for renewable and ''green''-energy resources is one of the most urgent challenges to the sustainable development of human civilization.[1,2] On the larger scale, besides the well-known energy resources that power the world today, such as petroleum, coal, hydroelectric, natural gas, and nuclear, active research and development are taking place into exploring alternative energy resources such as solar, geothermal, biomass, nuclear, wind, and hydrogen. At a much smaller scale, energy and technologies are desperately needed for independent, sustainable, maintenance-free, and continuous operation of implantable biosensors, ultrasensitive chemical and biomolecular sensors, nanorobotics, micro-electromechanical systems (MEMS), remote and mobile environmental sensors, security applications, and even portable/wearable personal electronics. A nanorobot, for example, is proposed as a smart machine that may be able to sense and adapt to the environment, manipulate objects, take actions, and perform complex functions, but a key challenge is to find a power source that can drive the nanorobot without adding much weight. An implanted wireless biosensor, for example, requires a power source, which may provide power directly or indirectly by charging of a battery. In general, the size of the battery is much larger than the size of the nanodevice, and this factor largely dictates the size of the entire system.

Near-future research involves the integration of multifunctional nanodevices into a nanosystem so that it can function as a living species with the capabilities of sensing, controlling, communicating, and actuating/responding. A nanosystem is composed of not only nanodevices but also a nanometer-sized power source (or ''nanobattery''). But the small size of the nanobattery largely limits the lifetime of the battery. It is highly desirable for wireless devices and even required for implanted biomedical systems to be self-powered without use of a battery; this can not only enhance the adaptability of the devices but also greatly reduce the size and weight of the system. Therefore, it is desirable to develop nanotechnology that harvests energy from the environment to self-power these nanodevices.[3] The goal of nanotechnology is to build self-powered nanosystems that are ultra-small in size, and exhibit super sensitivity, extraordinary multifunctionality, and extremely low power consumption. The resultant energy harvested from the environment should be sufficient to power the system.

[*] Prof. Z. L. Wang
School Materials Science and Engineering
Georgia Institute of Technology
Atlanta, Georgia 30332-0245 (USA)
E-mail: zhong.wang@mse.gatech.edu

[**] This work was supported by DOE BES, NSF, DARPA, and NASA. Thanks to the contributions from my group members: Dr. Jinhui Song, Dr. Xudong Wang, Dr. Yong Qin, Dr. Jin Liu, Dr. Jun Zhou, Dr. Rusen Yang, Yifan Gao, Peng Fei, Dr. Puxian Gao, Dr. Jr-Hau He, Dr. Changshi Lao, Dr. Yi-Feng Lin, and Wenjie Mai.

Scientists have developed various approaches for scavenging energy for mobile and wireless microelectronics using thermoelectrics, mechanical vibration, and piezoelectric vibration.[4,5] Photovoltaics, one of the most well-established energy-scavenging technologies, converts solar energy into electricity with the use of a photon–electron excitation process in semiconductor materials.[6] A human body provides numerous potential power sources—mechanical energy, vibrational energy, chemical energy (glucose), and hydraulic energy. If a small fraction of such energy sources could be converted into electricity, it may be sufficient to power small devices for biomedical devices.

2. Harvesting Mechanical Energy by Nanostructure-Enabling Technology: Why?

Photovoltaics, thermal electricity, and electromagnetic induction are the well-established technologies for energy harvesting. Why, though, do we need to harvest mechanical energy? We now consider the following occasions: In the case of individual sensors that are difficult to get to (e.g., in hostile territory) or if the sensor network consists of a large number of nodes distributed over a large geographical area, then it may not be possible to replace batteries when required. A self-sufficient power source, deriving its power from the environment and, thus, not requiring any maintenance, would be very desirable. In order for any system to be self-sufficient, it must harness its energy from its surrounding environment and store this harnessed energy for later use. A nanorobot, for example, is a smart machine that may be able to sense and adapt to the environment; however, it needs a power source that does not add much weight. If a nanorobot is placed in the body to perform sensing, diagnostic, and therapeutic action, one can easily introduce it into the body but it will be difficult or impossible to remove it to replace the battery. In the context of military sensing and surveillance, node placement may be in difficult-to-reach locations, may need to be hidden, or may be in dusty, rainy, dark or deep-forest environments. This precludes the use of solar-cell technologies as light is typically not available. Energy-harvesting methods applicable to the problem include systems that utilize random vibrations (e.g., vibrations near a roadway), temperature gradients (e.g., ground temperature is fairly constant at a point sufficiently below the surface), or any other phenomenon that could be exploited to provide energy. Clearly, it would be highly advantageous to develop technology to harvest mechanical energy.

3. Objectives of this Feature Article

In the last three years, we have explored innovative nanotechnology-enabled methods for converting mechanical energy (such as body movement, muscle stretching), vibrational energy (such as acoustic/ultrasonic waves), and hydraulic energy (such as body fluid and blood flows) into electrical energy, with the aim of building self-powered nanosystems.[7–10] This article provides a comprehensive review about our progress in developing the principle and technology of nanogenerators (NGs). We will focus on the fundamental mechanism of the NGs as supported by various experimental data. The core of our discussion is based on coupling the piezoelectric and semiconducting properties of ZnO nanowires/nanobelts (NWs/NBs) and the presence of a Schottky barrier at the metal–semiconductor interface. Rational designs for raising the output power of the NGs will be discussed. Finally, the new field of ''nanopiezotronics'' will be introduced, which will be used for fabricating a new class of electronic components, such as piezoelectric field-effect transistors (PE-FETs) and piezoelectric diodes (PE diodes) and sensors. The fundamental science presented is expected to serve as a guide and the foundation for future development. The future prospects of NGs and nanopiezotronics will be given.

4. Nanogenerators for Harvesting Mechanical Energy

4.1. The Concept of Piezoelectric Nanogenerators

The concept of the NG was first introduced by examining the piezoelectric properties of ZnO nanowires (NWs) with an

Zhong Lin Wang is a Regents' Professor, COE Distinguished Professor, and the director of the Center for Nanostructure Characterization at the Georgia Institute of Technology. He has authored and co-authored four scientific reference books and textbooks, over 520 peer-reviewed journal articles, 55 review papers and book chapters, edited and co-edited 14 volumes of books on nanotechnology, and holds 20 patents and provisional patents. Dr. Wang is in the top 25 most-cited authors in nanotechnology from 1992–2002 (ISI, Science Watch). His publications have been cited over 22 000 times. Dr. Wang discovered the nanobelt in 2001. He was elected fellow of the American Physical Society in 2005 and fellow of the AAAS in 2006. He received the 2001 S.T. Li Prize for Outstanding Contribution in Nanoscience and Nanotechnology, the 2000 and 2005 Georgia Tech Outstanding Faculty Research Author awards, and the 1999 Burton Medal from the Microscopy Society of America.

ADVANCED FUNCTIONAL MATERIALS

atomic force microscope.[7] ZnO has a wurtzite structure, in which the Zn cations and O anions form a tetrahedral coordination. ZnO has two important characteristics: One is the presence of polar surfaces, such as Zn^{2+}-terminated (0001) and O^{2-}-terminated $(000\bar{1})$. The interaction of the polar charges at the surface results in the growth of a wide range of unique nanostructures,[11] such as nanobelts,[12] nanosprings,[13] nanorings,[14] nanohelices.[15] Another characteristic is the lack of center symmetry, which results in a piezoelectric effect, by which a mechanical stress/strain can be converted into electrical voltage, and vice versa, owing to the relative displacement of the cations and anions in the crystal. It is important to point out that the polar surfaces are a surface effect, while piezoelectricity is an integrated volume effect. All of our studies in this Feature Article are based on piezoelectricity. Previous measurements have shown that ZnO NWs and nanobelts exhibit piezoelectricity, and the piezoelectric coefficient is even larger than that of the bulk.[16] Our first step is to find out if we can use ZnO NWs to convert mechanical energy into electricity and then effectively transport it through an external load.

As the first step of a proof of concept, our study is based on aligned ZnO NWs grown on a conductive solid substrate (Fig. 1a).[17–19] The measurements were performed by atomic force microscopy (AFM) using a Si tip coated with a Pt film. In the AFM contact mode, a constant normal force of 5 nN was maintained between the tip and sample surface (Fig. 1b). The tip scanned over the top of the ZnO NW, and the tip's height was adjusted according to the surface morphology and local contacting force. In the corresponding voltage-output image for each contact position, many sharp output peaks were observed (Fig. 1c). Note the voltage signal was inverted for display purposes: it is actually negative in reference to the grounded end. By examining the topological profile of an NW and its corresponding output potential, a delay was observed for the voltage output signal (Fig. 1d), which means that there was no electric power output when the tip was first in contact with the NW, but a sharp voltage peak was generated at the moment when the tip was about to break contact with the NW. This delay is a key signature of the power-output process. It is important to note that the voltage V_L presented here was converted from the current flowing through the external load of resistance R_L. The NG based on the ZnO NWs has the following experimental characteristics:

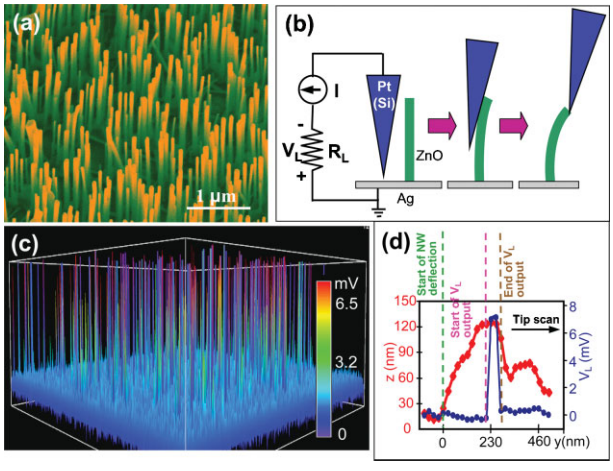

Figure 1. a) Scanning electron microscopy (SEM) images of aligned ZnO NWs grown on a GaN/sapphire substrate. b) Experimental setup and procedure for generating electricity by deforming a piezoelectric NW using a conductive AFM tip. The AFM scans across the NW arrays in contact mode. c) Output-voltage image of the NW arrays when the AFM tip scans across the NW arrays. d) An overlap plot of the AFM topological image (red line) and the corresponding generated voltage (blue line) for a single scan of the tip across an NW. A delay in the electricity generation is apparent [7].

i) The output potential is a sharp peak that is negative in reference to the grounded end of the NW.
ii) No output current is received when the tip first touches the NW and pushes the NW; electrical output is observed only when the tip is about to leave the NW at the second half of the contact.
iii) The power output occurs only when the tip touches the compressive side of the NW.[20]
iv) An output signal is observed only for piezoelectric NWs. No electrical output is received if the NWs are tungsten oxide, carbon nanotubes, silicon, or metal. Friction or contact potential plays no role in the observed output power.[20]
v) The magnitude of the output signal is highly sensitive to the size of the NWs.[21]
vi) To effectively output electricity, the contact between the tip and the NW is required to be Schottky in nature, and the contact between the NW and ground is ohmic.

Positive output voltage peaks have been observed for CdS NWs under visible-light illumination[22] and ZnO NWs coated with a p-type polymer.[23] This is due to a change in contact transport characteristic from Schottky to quasi-ohmic.

4.2. Piezoelectric Potential at Surfaces of a Bent Nanowire

To have a better understanding about the piezoelectric voltage output from a single NW, we need to first calculate the magnitude of the potential created in an NW when it is subject to mechanical deformation. We have applied a continuum model for the electrostatic potential in a laterally bent NW.[24] Our theoretical objective is to derive the relationship between the potential distribution in the NW and the dimensionality of the NW and magnitude of the applied force at the tip. For this purpose, we start from the governing equations for a static piezoelectric material, which are in four sets: mechanical equilibrium equation (Eq. 1), constitutive equation (Eq. 2), geometrical compatibility equation (Eq. 3), and Gaussian equation of electric field (Eq. 4). The mechanical equilibrium condition when there is no body force $\vec{f}_e^{(b)} = 0$ acting on the nanowire is:

$$\nabla \cdot \sigma = \vec{f}_e^{(b)} = 0 \tag{1}$$

where σ is the stress tensor, which is related to strain ε, electric field $\vec{E}$, and electric displacement $\vec{D}$ by constitutive

equations:

$$\begin{cases} \sigma_p = c_{pq}\varepsilon_q - e_{kp}E_k \\ D_i = e_{iq}\varepsilon_q + \kappa_{ik}E_k \end{cases} \quad (2)$$

Here c_{pq} is the linear elastic constant, e_{kp} is the linear piezoelectric coefficient, and κ_{ik} is the dielectric constant. The compatibility equation is a geometrical constraint that must be satisfied by strain ε_{ij}:

$$e_{ilm}e_{jpq}\frac{\partial^2 \varepsilon_{mp}}{\partial x_l \partial x_q} = 0 \quad (3)$$

In Equation 3 the indices are in the normal definition and Nye notation is not used. e_{ilm} and e_{jpq} are Levi–Civita antisymmetric tensors. For simplicity of the derivation, we assume that the NW bending is small. Finally, by assuming no free charge $\rho_e^{(b)}$ in the nanowire, which assumes that the ZnO nanowire has no conductivity, the Gaussian equation must be satisfied:

$$\nabla \cdot \vec{D} = \rho_e^{(b)} = 0 \quad (4)$$

We have developed a perturbation theory for solving Equations 1–4 analytically.[24] Under the different orders of approximations, these equations correspond to the decoupling and coupling between the electric field and mechanical deformation: the 0^{th} order solution is purely mechanical deformation without piezoelectricity; the 1^{st} order is the result of a direct piezoelectric effect, whereby strain–stress generates an electric field in the NW; and the 2^{nd} order shows up the first feed back (or coupling) of the piezoelectric field to the strain in the material. In our case for an NW bent by an AFM tip, the mechanical deformation behavior of the material is almost unaffected by the piezoelectric field in the NW. Therefore, for the calculation of piezoelectric potential in the nanowire, the 1^{st} order approximation may be sufficient.

In the configuration of the nanogenerator, the root end of the nanowire is affixed to a conductive substrate, while the top end is pushed by a lateral force f_y. If the nanowire is approximated as a cylindrical shape with radius a, and in cylindrical coordinates, the piezoelectric potential inside and outside the NW is:

$$\varphi = \begin{cases} \frac{1}{8\kappa_\perp}\frac{f_y}{I_{xx}E}[2(1+\nu)e_{15}+2\nu e_{31}-e_{33}]\left[\frac{\kappa_0+3\kappa_\perp}{\kappa_0+\kappa_\perp}\frac{r}{a}-\frac{r^3}{a^3}\right]a^3\sin\theta, r<a \\ \frac{1}{8\kappa_\perp}\frac{f_y}{I_{xx}E}[2(1+\nu)e_{15}+2\nu e_{31}-e_{33}]\left[\frac{2\kappa_\perp}{\kappa_0+\kappa_\perp}\frac{a}{r}\right]a^3\sin\theta, r\geq a \end{cases} \quad (5)$$

where $I_{xx} = \pi a^4/4$, κ_0 is the permittivity in a vacuum, E is the elastic modulus, $\kappa_\perp$ is the dielectric constant in the basal plane, ν is the Poisson ratio. The maximum potential at the surface ($r = a$) of the NW at the tensile (T) side ($\theta = -90°$) and the compressive (C) side ($\theta = 90°$), respectively, becomes:

$$\varphi_{\max}^{(T,C)} = \pm\frac{1}{\pi}\frac{1}{\kappa_0+\kappa_\perp}\frac{f_y}{E}[e_{33}-2(1+\nu)e_{15}-2\nu e_{31}]\frac{1}{a} \quad (6)$$

Or alternatively,

$$\varphi_{\max}^{(T,C)} = \pm\frac{3}{4(\kappa_0+\kappa_\perp)}[e_{33}-2(1+\nu)e_{15}-2\nu e_{31}]\frac{a^3}{l^3}v_{\max} \quad (7)$$

where $v_{\max}$ is the maximum deflection of the NW at the tip. The maximum potential at the surface of the NW is directly proportional to the lateral displacement of the NW and inversely proportional to the cubic square of its length-to-diameter aspect ratio.

In the first case, the ZnO wire diameter is $d = 50$ nm, length is $l = 600$ nm, and lateral force applied by AFM tip is 80 nN; therefore, the magnitude of piezoelectric potential is 0.3 V at the stretched surface and is −0.3 V at the compressive surface (Fig. 2). The result of the analytical equation (Eq. 5) is less than 5% away from the results calculated by finite elements. Although such calculation was made by assuming that the NW was an insulator, it at least gives a magnitude of the piezoelectric potential. Our recent calculation, which includes finite conductivity of the NW, gives a consistent result.

The calculation shows that the piezoelectric potential in the NW almost does not depend on the z-coordinate along the NW unless very close to either end, meaning that the NW can be approximately taken as a "parallel-plate capacitor". This is the basis of the proposed nanopiezotronics in Section 5.

The voltages at the stretched and compressed sides of the NW have been measured by using a metal tip that is placed either at the tensile side or the compressive side of the NW, while the NW is deflected by air blowing.[25] When a periodic gas flow pulse was applied to a ZnO wire, the wire was bent and a corresponding periodic negative voltage output (Fig. 3a) was detected by connecting the surface of the compressed side of the NW to an external measurement circuit. The voltage output detected here was −25 mV. Correspondingly, a periodic positive voltage output (Fig. 3b) was detected at the stretched side of the wire, by using a Au-coated needle, when the ZnO wire was periodically pushed by the Au-coated needle. Such measurements were done with the use of a voltage amplifier.

The measured voltage signal in our experiment is much lower than that predicted by the static model calculation (see

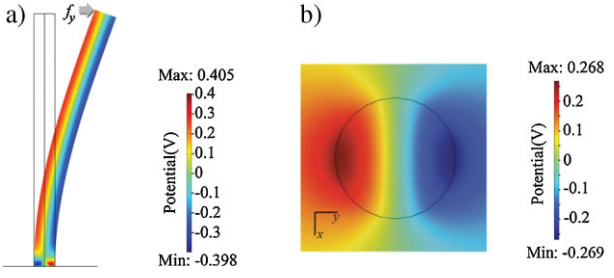

Figure 2. Calculated potential distribution for a ZnO nanowire with diameter $d = 50$ nm and length $l = 600$ nm at a lateral bending force of 80 nN. a) Side and b) top cross-sectional (at $z_0 = 300$ nm) output of the piezoelectric potential [24].

ADVANCED FUNCTIONAL MATERIALS

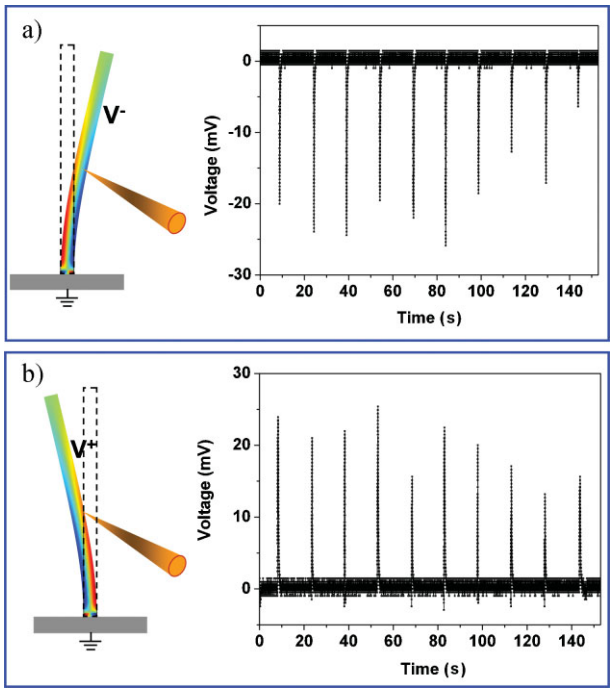

Figure 3. Direct measurements of the asymmetric voltage distribution on the tensile and compressive side surfaces of a ZnO wire. a) By placing a metal tip at the right-hand side and blowing Ar pulses at the left-hand side, negative voltage peaks of approximately 25 mV were observed once the pulse was on. b) By quickly pushing and releasing the wire at the right-hand side by a metal tip, a positive voltage peak of approximately 25 mV was observed for each cycle of the deflection. The frequency of the deflection was once every 15 s [25].

Fig. 2). The following reasons may account for this difference. First of all, the contact resistance can be very large as a result of the small contact area between the ZnO wire and the tip. Therefore, the voltage created by the piezoelectric effect of the ZnO wire was largely consumed at the contact due to the contact resistance,[26] and only a small portion was received as the output. Secondly, the capacitance of the measurement system could be much larger than the capacitance of the ZnO wire. The large system capacitance consumes most of the charge produced by the ZnO wire and results in a lower voltage output. Finally, the finite conductivity of ZnO may greatly reduce the magnitude of the piezoelectric potential.[27]

It must be pointed out that the voltage measured across the load is negative in reference to the grounded electrode. This means that the current flows from the tip into the NW. This is a common and important signature of the NG presented here.

4.3. Schottky Barrier at the Electrode–Nanowire Interface

The Schottky contact between the metal contact and ZnO NW is another key factor affecting the current generation and output process. To examine the role played by the Schottky barrier in the NG, we used an AFM-based manipulation and measurement system as used in our first study for demonstrating the piezoelectric NG (see Fig. 4a). When a 100 nm thick Pt-coated Si tip was used for scanning the NWs in contact mode, voltage peaks were observed (Fig. 4b), and the output voltage was in the order of −11 mV (the negative sign means that the current flowed from the grounded end through the external load). By changing the tip to an Al–In (30 nm/30 nm) alloy-coated Si tip, the ZnO NWs showed no piezoelectric output (Fig. 4c). To understand these two distinct performances, we have measured their corresponding *I–V* characteristics with the ZnO NWs. To ensure the stability of the contact, we used a large electrode that was in contact with a group of NWs, as shown in Figure 4d. The Pt–ZnO contact clearly presented a Schottky diode (Fig. 4e), while the AlIn–ZnO was an ohmic contact. In reference to the piezoelectric output presented in Figure 4b and c, we conclude that a Schottky contact between the metal electrode and ZnO is necessary for a working NG.[28]

By tuning the height of the Schottky barrier and the density of charge carriers in ZnO using UV illumination, the output of an NG has been largely changed.[28] No voltage/current is generated if there is no Schottky barrier at the tip/electrode–ZnO interface.

4.4. The Charge Generation and Output Process of a Piezoelectric Nanowire

The physical principle for creating, separating, accumulating, and outputting the piezoelectric potential in the NW is a coupling of the piezoelectric and semiconducting properties of the material.[7,20] For a vertically straight ZnO NW, the deflection of the NW by the AFM tip creates a strain field, with the outer surface being tensile (positive strain ε) and the inner surface compressive (negative strain ε). The asymmetric strain introduces an asymmetric potential at the two surfaces, with the compressed surface having negative V^- ($=\varphi^C$) and the tensile surface positive V^+ ($=\varphi^T$).

We now consider the power-output process. In the first step, the AFM conductive tip that induces the deformation is in contact with the tensile surface of positive potential V^+ (Fig. 5a). The Pt metal tip has a potential of nearly zero, $V_m = 0$, so the metal tip–ZnO interface is negatively biased for $\Delta V = (V_m - V^+) < 0$. By consideration of the n-type semiconductor characteristic of the as-synthesized ZnO NWs, the Pt metal–ZnO semiconductor (M–S) interface, in this case, is a reverse-biased Schottky diode, and little current flows across the interface. This is the process of creating, separating, and accumulating the piezoelectric charges. In the second step, when the AFM tip is in contact with the compressed side of the NW (Fig. 5b), the metal tip–ZnO interface is positively biased for $\Delta V = V_L = (V_m - V^-) > 0$. The M–S interface in this case is a positively biased Schottky diode, and it produces a sudden increase in the output electric current. The current is the result of ΔV driven flow of electrons from the semiconducting ZnO NW to the metal tip. This is the power-output process.

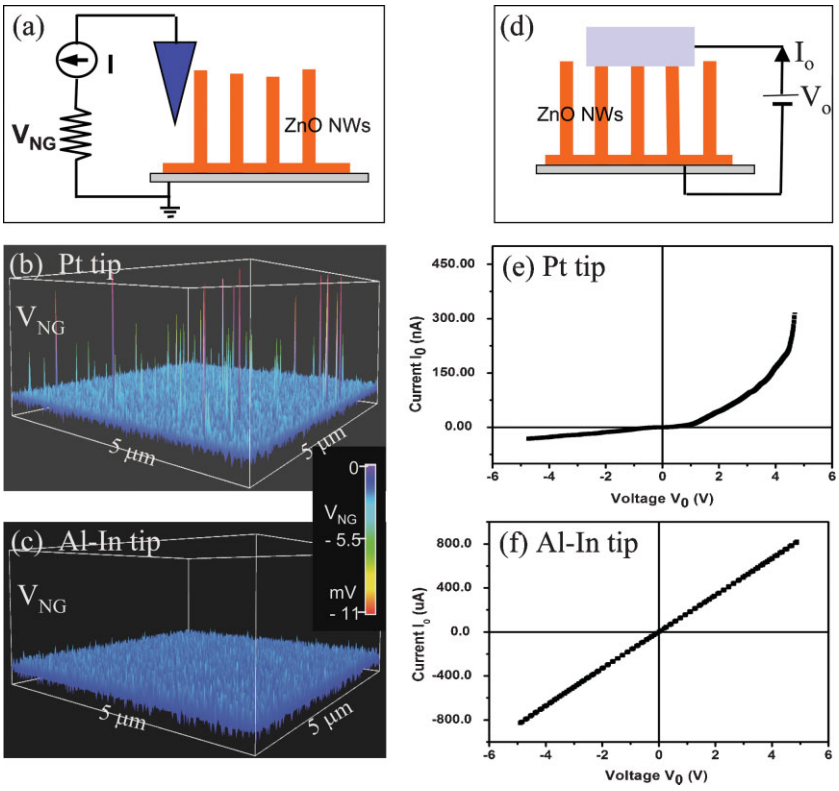

Figure 4. a) AFM-based measurement setup for correlating the relationship between the metal–ZnO contact and the NG output. b) Output potential generated by ZnO NW array when scanned by a Pt-coated Si tip. c) No output potential is generated by ZnO NW array when scanned by an Al–In-coated Si tip. d) Experimental setup for characterizing the *I–V* characteristics of a metal–ZnO NW contact. e) *I–V* curve of a Pt–ZnO NW contact, showing the Schottky diode effect. f) *I–V* curve of an alloyed AlIn–ZnO NW contact, showing ohmic behavior [28].

We now consider the nature of the piezoelectric potential. The piezoelectric potential is created by the polarization of ions in the crystal rather than the free, mobile charges. Since the charges associated with the ions are rigid and affixed to the atoms, they cannot freely move. Free carriers in the semiconductor NW may screen the piezoelectric charges, but they cannot completely deplete the charges. This is a distinct difference from the p–n junction in semiconductor physics. Therefore, the piezoelectric potential is still preserved, although a possible reduction in magnitude is possible owing to the finite conductivity of the NW.

An as-synthesized ZnO NW is generally n-type. The presence of oxygen vacancies and impurities and a large portion of surface atoms (surface states) naturally introduces a moderate conductivity to the NW. These free carriers can partially screen the piezoelectric charges, but they cannot entirely neutralize the charges. Therefore, the piezoelectric potential is still preserved, at a reduced magnitude, even when the moderate conductivity of ZnO is considered.

We now present an explanation of the charge-releasing process for an NG based on the band structure model. The AFM tip (T) has a Schottky contact (barrier height Φ_{SB}) with the NW, while the NW has an Ohmic contact with the grounded side (G) (Fig. 6a). When the tip slowly pushes the NW, a positive piezoelectric potential V^+ is created at its tensile surface. As the tip continues to push the NW, electrons slowly flow from the grounded electrode through the external load to reach the tip, but the electrons cannot pass across the tip–NW interface because of the presence of a reverse-biased Schottky barrier at the contact (Fig. 6b). In such a case, the accumulated free charges at the tip may affect the piezoelectric potential distribution in the NW because of the screening effect of the charge carriers. The piezoelectric potential is generated as a result of the rigid and non-mobile ionic charges in the NW; the potential cannot be completely depleted by the free carriers. The local, newly established potential V'^+ lowers the conduction band (CB) slightly.

When the tip scans in contact mode across the NW and reaches the middle point of the NW (see Fig. 6c), the local piezoelectric potential is zero. In such a case, with a sudden drop in local potential, the originally accumulated electrons in the tip flow back through the load to the ground. This process is faster than the charge-accumulation process presented in Fig. 6b. An alternative but similar result is that the tip temporarily lifts off the NW, which also leads to the back flow of the accumulated electrons to the ground.

When the tip reaches the compressive side of the NW (Fig. 6d), the local potential drops to V''^- (negative), which results in the raising of the conduction band near the tip. If the raise in local potential energy is large enough to overcome the Schottky barrier threshold at forward bias, as determined by the degree of NW bending, the local accumulated n-type carriers in the NW can quickly flow through the contact to the tip, which creates a circular flow of the electrons in the external circuit, thus producing a current. This process is a lot faster than the charge-accumulation process; therefore, the created transient potential at the external load is large enough to be detected beyond the noise level. The presence of a Schottky contact at the tip–NW interface is mandatory for an NG, which acts like a "gate" for separating and slowly accumulating the charges and then quickly releasing them. The absence of a "gate" at an Ohmic contact results in no charge accumulation or release; thus, no detectable signal will be received.

The next question is how large is the output voltage? This question can be answered by the energy-band diagram shown in Figure 6e for the NG. The role played by the piezoelectric potential is to drive the electrons from the ZnO NW, overcoming the threshold energy at the metal–ZnO interface, into the Pt electrode but it does not directly determine the magnitude of the output voltage. As more electrons are being

ADVANCED FUNCTIONAL MATERIALS

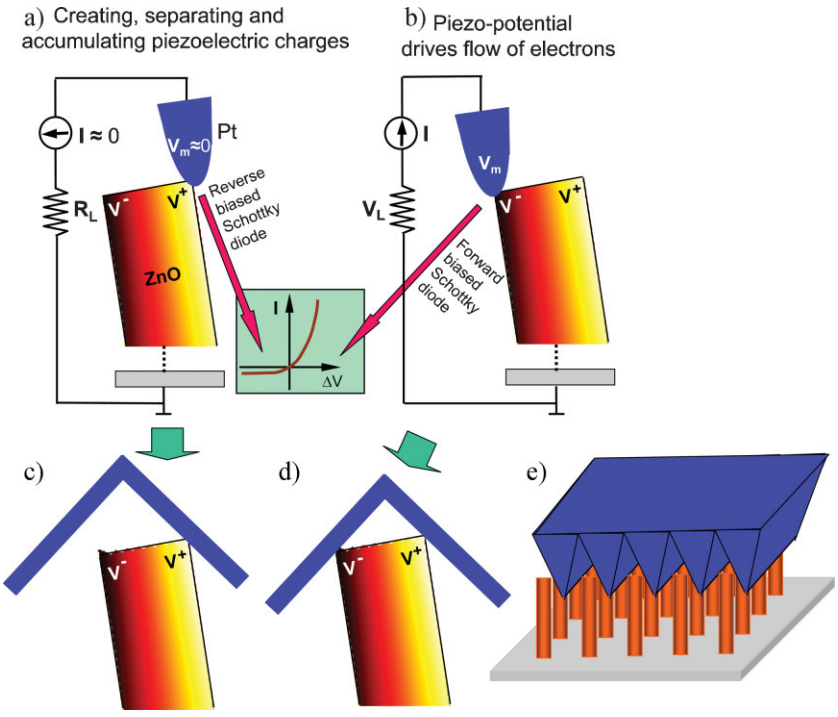

Figure 5. Physical principle of the observed power-generation process of a piezoelectric ZnO NW, showing a unique coupling of piezoelectric and semiconducting properties in this metal–semiconductor Schottky-barrier-governed transport process. a,b) Metal and semiconductor contacts between the AFM tip and the semiconductor ZnO NW at two reversed local contact potentials (positive and negative), showing reverse- and forward-biased Schottky rectifying behavior, respectively. The Schottky barrier is responsible for separating, accumulating, and later releasing the charges [7]. c,d) Schematic idea for replacing the role played by an ATM tip by an "inverted-V shaped" electrode. e) The idea of introduction of a zigzag electrode to form hundreds of parallel tips, each acting like an AFM tip [8].

"pumped' into the Pt electrode, the local Fermi surface is suddenly raised. Therefore, the output voltage is the difference between the Fermi energies of Pt and the bottom Ag electrode (5–30 mV depending on NW size and degree of bending). In practice, the measured voltage at load must consider contact resistance.

It must be pointed out that, although the total amount of charge Q generated by a single NW is small (ca. 1000–10 000 electrons), quick release of these electrons can produce a significantly large electric current/voltage pulse, because $V_L \approx R_L Q/\Delta t$, where Δt is the time interval for the charge-releasing process. A conventional calculation of the output voltage by the capacitance C of the NWs and system ($V = Q/C$) applies only to the static process! The voltage predicted by this calculation is usually far less than the magnitude of the pulse observed experimentally.

As a summary of the charge-flowing processes presented in Figure 6, the first process is a forward and back flow of the electrons through the load from the ground to the tip; the second process is a piezoelectric-potential-driven circular flow of the electrons through the NW. The two processes generate constructive currents flowing in the same direction, resulting in a negative voltage at the load in reference to the grounded electrode. This is an important characteristic. The output current can be significantly large if the charge-releasing process is fast. In the case of the AFM tip contact, the second process is likely the dominant process. The entire process of energy generation can be summarized into one sentence: the piezoelectric-potential-driven flow of external electrons is the power-output process of the nanogenerator.

4.5. Direct-Current Nanogenerator Driven by an Ultrasonic Wave

Although the approach presented in Figure 2 has demonstrated the concept of the NG, for technological applications, we must make an innovative design to drastically improve the performance of the NG in the following aspects. First, we must eliminate the use of AFM for making the mechanical deformation of the NWs so that the power generation can be achieved by an adaptable, mobile, and cost-effective approach over a larger scale. Secondly, all of the NWs are required to generate electricity simultaneously and continuously, and all of this electricity should be effectively collected and outputted. Finally, the energy to be converted into electricity has to be provided in the form of a wave or vibration from the environment, so the NG can operate "independently" and wirelessly. We have developed an innovative approach that has addressed these challenges.[8]

To replace the role played by the AFM tip in deflecting the NW, we first examined an "inverted V-shaped" (i-V) electrode. Once the i-V electrode moves downward as driven by an external excitation, an NW would be deflected towards the left, for example. At the first contact point, a positive potential is created by the local tensile strain (Fig. 5c). In such a case, the piezoelectric potential is preserved as the local contact is a reverse-biased Schottky barrier that does not permit the flow of charge. When the electrode further pushes the NW until it bends enough to reach the other side of the i-V electrode (Fig. 5d), the local contact is a forward-biased Schottky barrier, thus, the local potential drop drives the flow of electrons. Therefore, we can replace the AFM tip by an i-V electrode. The i-V electrode can be extrapolated into a zigzag electrode (Fig. 5e) made of Si coated with Pt. The Pt coating is not only for enhancing the conductivity of the electrode but also for creating a Schottky contact at the interface with ZnO. In practice, the coating metal can be any conductive alloy as long as it can form a Schottky barrier with ZnO. The zigzag electrode acts as an array of parallel AFM tips. The electrode was placed and manipulated above the NW arrays at a controlled distance. The output electricity produced by the

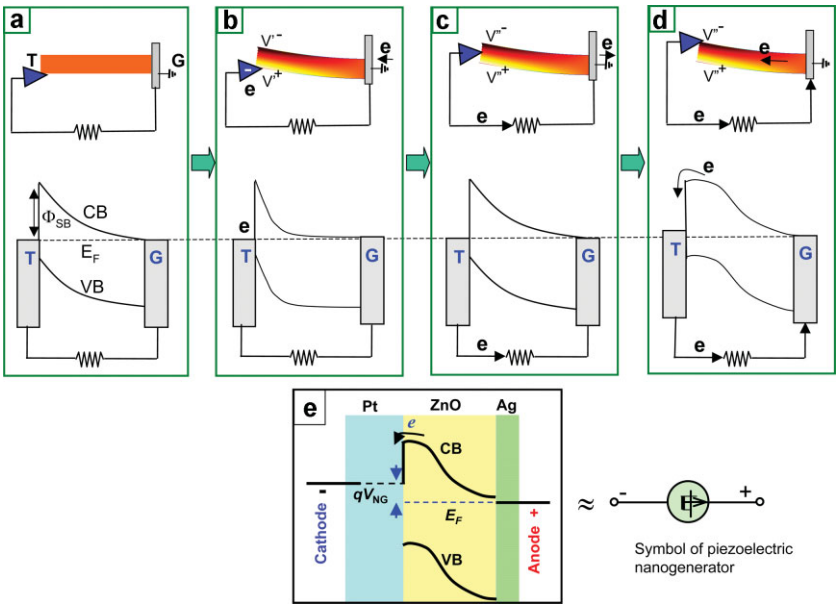

Figure 6. Band diagram for understanding the charge output and flow processes in a nanogenerator. a) Schematic and energy diagram of an NW with one end grounded (G) and the other end to be pushed by a conductive AFM tip (T). A Schottky barrier is at the tip–NW interface. b) Once it is slowly deflected, the asymmetric piezoelectric potential in the NW changes the profile of the conduction band (CB; valence band: VB). The local positive piezoelectric potential at the contact area results in a slow flow of electrons from ground through the load to the tip. The electrons will accumulate in the tip. c) When the tip scans across the NW and reaches its middle point, a drop in local potential to zero results in a back flow of the accumulated electrons through the load to ground. d) Once the tip reaches the compressive surface, a local negative piezoelectric potential raises the profile of the conduction band. If the piezoelectric potential is large enough, electrons in the n-type ZnO NW can flow to the tip. This circular motion of the electrons in the circuit is the output current. e) Energy-band diagram for the NG, presenting the output voltage and the role played by the piezoelectric potential. The diagram on the right-hand side is the symbol designed to represent a piezoelectric nanogenerator.

relative deflection/displacement of the NWs and the electrode via bending or vibration is expected to be simultaneous and continuous.

Figure 7a–c shows four possible configurations of contact between an NW and the zigzag electrode. NWs I and II are being deflected towards the left and right sides, respectively, by the electrode. Regardless of their deflection directions, the currents produced by NWs I and II constructively add up. NW III is chosen to elaborate the vibration induced by an ultrasonic wave. As shown in Figure 7c, when the compressive side of NW III is in contact with the electrode, the same discharge process as for NW I occurs, resulting in the flow of current from the electrode into the NW. NW IV, short in height, is under compressive strain by the electrode without bending. In such a case, the piezoelectric voltage created at the top of the NW is negative. Thus, across the electrode–ZnO interface, a positively biased Schottky barrier is formed; hence, the electrons can freely flow across the interface. As a result, electrons flow from the NW into the top zigzag electrode as the deformation occurs. This discharging process, if significant, may also contribute to the measured current. The output current is a sum of those NWs that actively contribute to the output power, but the voltage of the NG is determined by a single NW because all of the NWs are ''in parallel''.

The packaged NG was placed in a water bath to measure the closed-circuit current (I_{sc}) and open-circuit voltage (V_{oc}). An ultrasonic wave of frequency 41 kHz was periodically turned on every other 15 s. Figure 7e shows the closed-circuit current when the ultrasonic wave was turned on and off. The data clearly indicates that the current output originates from the NG as a result of ultrasonic wave excitation as the output coincides with the working cycle of the ultrasonic wave generator. A similar pattern in the open-circuit voltage output was also observed, as shown in Figure 7f. Both current and voltage outputs exhibit high levels for this type of NG, with values of approximately 500 nA and 10 mV, respectively. Considering the effective area of the NG (6 mm^2), it is equivalent to a current generation density of ca. 8.3 $\mu A\,cm^{-2}$. A power generation density of about 83 $nW\,cm^{-2}$ is reported,[26] which shows great potential to power nanosensors.

It must be pointed out that operation of the NG does not rely on mechanical resonance as required by some energy-harvesting technologies, instead it is based on mechanical deflection. Such a design allows the NG to work in a wide range of frequencies, from a few hertz, to kilohertz, and even to megahertz magnitudes. This large adaptability greatly expands the application of the NG for harvesting various mechanical energies.

4.6. Criteria for Identifying the True Output Signal from a Nanogenerator

Measurement of the current and voltage signal generated by an NG is rather challenging, especially at the level of nanoamperes and millivolts, because of system and/or environmental interference, such as system capacitance, thermal/instability drifting, and the bias of the amplifier. The electrical measurements of NGs is even more complex than conventional conductivity measurements, because we are looking for the current/voltage that is generated by the NGs rather than the bias current/voltage introduced by the electrical measurement system that is detecting the signals. Another challenge comes from the mechanical movement of the components during energy conversion, which could introduce electronic interference and capacitance change. The most frequent problems for an inexperienced researcher are that they observe no electrical output or no electrical signal for any sample they use. Both unusual cases are probably complicated by artifacts. Extreme caution must be exercised in each step to

ADVANCED FUNCTIONAL MATERIALS

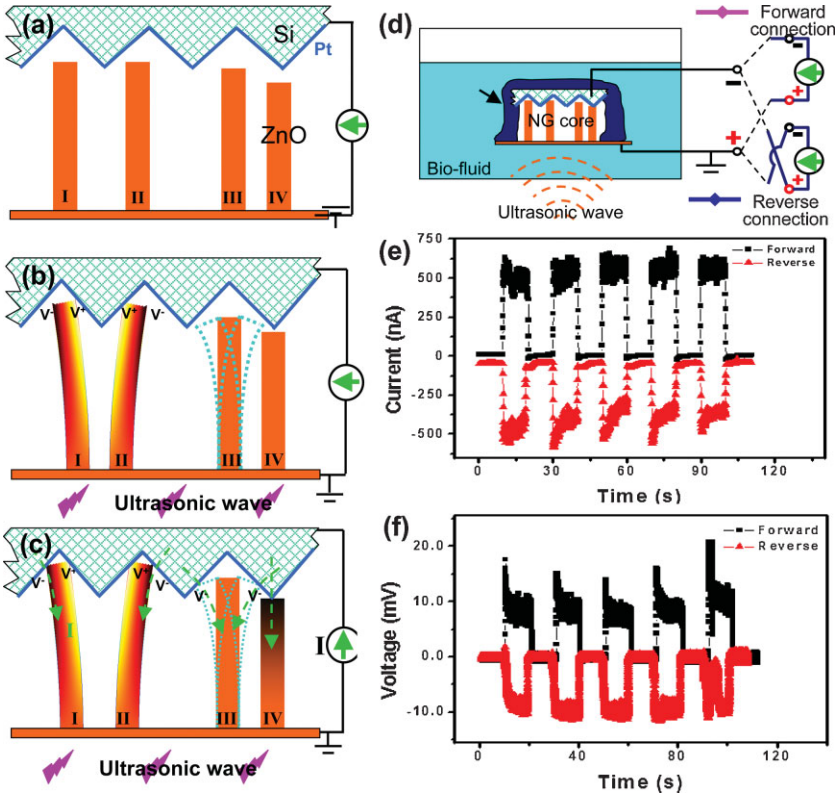

Figure 7. The mechanism of the NG driven by an ultrasonic wave [8]. a) Schematic illustration of the zigzag electrode and the four types of NW configurations. b) The piezoelectric potential created across NWs I and II under the push/deflection of the electrode but without flow of current because of the reverse-biased Schottky barrier at the electrode–NW interface. NW III is in vibration under the stimulation of the ultrasonic wave. NW IV is in compressive strain without bending. c) Once the NWs touch the surface of the adjacent teeth, the Schottky barrier at the electrode–NW interface is forward biased, piezoelectric discharge occurs, resulting in the observation of current flow in the external circuit. d) Schematic of an NG that operates in a biofluid and the two types of connections used to characterize the performance of the NG. The black and red curves represent signals from forward and reversely connected current/voltage (I/V) meters, respectively. e,f) The short-circuit current and open-circuit voltage measured by the two types of connections when the ultrasonic wave was periodically turned on and off [29].

ensure the signal was generated by the NG instead of the measurement circuits. In many cases, we have built simulating circuits to identify the sources of artifacts. The key for each measurement is to repeat it for many devices and under different experimental conditions. In the last three years, we have developed two testing criteria to identify the true signal from an NG. One must also carefully check the specification of the measurement system to ensure it has an extremely small capacitance (~pf), low noise (< 0.5 mV), and very low bias current (< 2 pA).

The first criterion is the "switching-polarity" test.[29] As illustrated in Figure 7d, the current/voltage meter is first forward connected, for example, positive and negative probes were connected to the positive and negative electrodes, respectively. Then the connection polarity to the two electrodes of the NG was reversed. The corresponding I_{sc} and V_{oc} signals are shown in Figure 7d and e, respectively. A switch in sign in both current and voltage after switching the connecting polarity is a key test to eliminate the effects from measurement system error and confirm that the power is generated by the NG. Resistors and capacitors are symmetric devices and they cannot produce a reversal in output signal if it is initiated from the measurement system. A diode can only produce a one-way current signal but zero in the other direction, which cannot result in a reversed current if it originates from the measurement system.

The second criterion is a linear superposition of the output current/voltage when two or more NGs are connected in parallel/series.[29] As shown in Figure 8a and b, two NGs I and II have been measured under the same experimental conditions. NG I produced an average I_{sc} of about 0.7 nA and NG II generated a signal of 1 nA. These two NGs were then connected in parallel (inset of Fig. 8c) and tested under the same conditions again. The resultant output current reached an average of about 1.8 nA, which is the sum of the two individual outputs (Fig. 8c). This concept was further proved by antiparallel connection of NG I and NG II (inset of Fig. 8d). Since the magnitude of I_{sc} for the two NGs was very close, the total current was mostly cancelled out by the "head-to-tail" connection in parallel, and the received signal was around the baseline (Fig. 8d), just as expected.

Capacitors, resistors, and inductors are symmetric devices and their output is equivalent regardless of which direction the current flows. However, diodes are nonsymmetric devices. Once a diode is involved, one must demonstrate the "add-up" and "subtract-off" tests as illustrated above for identifying the true signals generated by the NGs. Figure 8f and g summarizes the eight connection configurations and the expected results for ruling out artifacts. These tests are essential for identifying the true output from NGs.

For technological applications, raising the voltage and current outputs of the NG is essential for raising the output power. If we take each NG as a "battery", the most straightforward approach for increasing the current/voltage is to put them in parallel/series, respectively.

A Schottky barrier is required between the zigzag electrode and the NWs. By simply measuring the I–V characteristics of a packaged NG, one can use the presence of a Schottky barrier as a criterion for identifying a working NG verses a defected one.[28] This is useful for quality inspection and control.

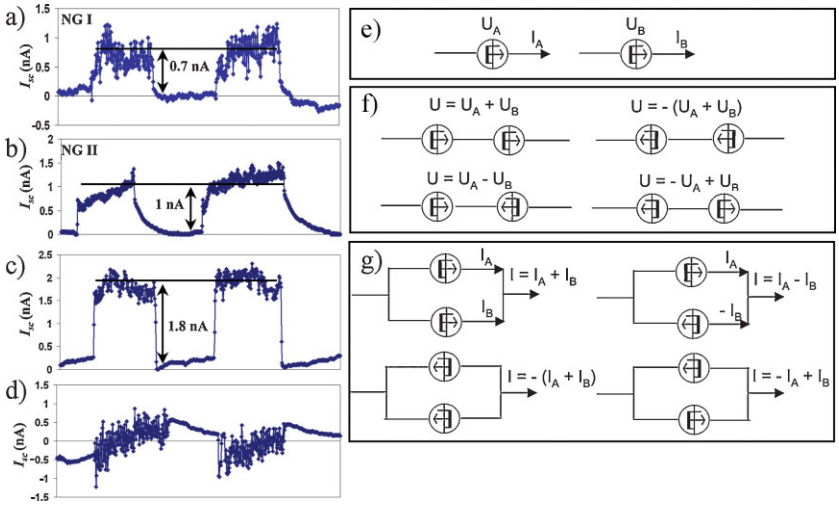

Figure 8. Criteria adopted for differentiating between the true output signal versus that from artifacts. a,b) Current signal measured from two individual NGs, I and II. c,d) Current signal measured from parallel and antiparallel connected NG I and NG II, respectively [29]. e) Two NGs with expected output. The symbol presented here represents the piezoelectric NG. f) Four testing configurations for serial connection of two NGs to identify true voltage output signals. g) Four testing configurations for serial connection of two NGs to identify true current output signals.

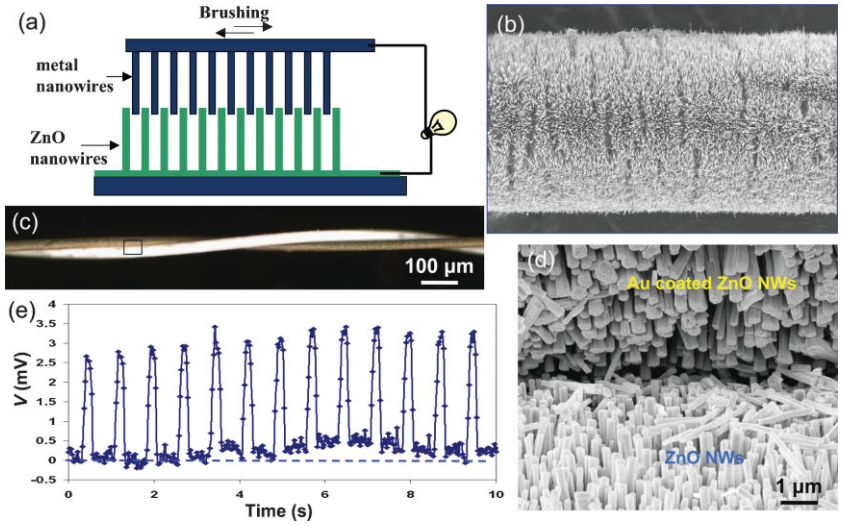

Figure 9. The design and mechanism of the fiber-based NG as driven by a low-frequency, external vibration/friction/pulling force. a) Schematic idea of ''two-brush'' NG. One brush is made of ZnO nanowires, and the other brush is metal nanowires. b) SEM image showing the distribution of NWs grown on a fiber surface. c) An optical micrograph of a pair of entangled fibers, one of which is coated with Au (in darker contrast). d) SEM image at the ''teeth-to-teeth'' interface of two fibers covered by NWs, with the top one coated with Au. The Au-coated NWs serve as the conductive ''tips'' that deflect the NWs at the bottom: a piezoelectric–semiconducting coupling process generates electric current. e) The piezoelectric potential output by the two-fiber NG under the pulling and releasing of the top fiber by an external force [9].

4.7. Fiber-Based Nanogenerators As Flexible and Foldable Power Sources

The ceramic or semiconductor substrates used for growing ZnO NWs are hard, brittle, and cannot be used in areas that require a foldable or flexible power source, such as implantable biosensors in muscles or joints, and power generators built into walking shoes.[30] It is necessary to use conductive polymers, which are likely to be biocompatible and safe, as substrates. Two advantages are offered by this approach. One is the cost-effective, large-scale solution to grow ZnO NW arrays at a temperature below 80 °C. The other is the large degree of choice of flexible plastic substrates for growing aligned ZnO NW arrays, which could play an important role in flexible and portable electronics for harvesting low-frequency (ca. 10 Hz) energy from the environment, such as from body movement (e.g., gestures, respiration, or locomotion).

We have recently demonstrated fiber-based NGs.[9] The design of the NG is based on the zigzag-electrode mechanism, but we have replaced the zigzag electrode by an array of metal wires, as shown in Figure 9a. By brushing the metal NW arrays across the ZnO NW arrays, the metal wires act like an array of AFM tips that induce the mechanical deformation to the ZnO nanowires and collect the charges. A unique advantage for ZnO NW arrays is that they can be grown at 80 °C on substrates of any shape and any material. In reality, the metal NW arrays were made by metal coating of ZnO nanowire arrays grown on Kevlar fibers (Fig. 9b). In practice, any fiber should work as long as it has good electrical conductivity. The metal to be coated is required to form a Schottky contact with ZnO. Entangling the two fibers, one coated with Au and one without, sets the principle of the fiber-based NG (Fig. 9c). The NWs on the two fibers are ''teeth-to-teeth'' (Fig. 9d), a relative deflection by a distance as short as one NW size is sufficient to generate electricity. A cycled relative sliding between the two fibers produces output voltage and current owing to the deflection and bending of the ZnO nanowires (Fig. 9e). This is the fiber-based NG,[9] with potential for harvesting energy from body movement, muscle stretching, light wind, and vibration. It establishes the basis for building a ''power-shirt'' to wear.

5. Nanopiezotronics

The concept of nanopiezotronics was first introduced in 2006,[31] and its definition and detailed description were

ADVANCED FUNCTIONAL MATERIALS

published in 2007.[32,33] The basis of nanopiezotronics is to use the coupled piezoelectric and semiconducting properties of nanowires and nanobelts for designing and fabricating electronic devices and components, such as field-effect transistors and diodes. We now illustrate a few components of such devices, based on which we will introduce the principle of piezotronics.

5.1. Piezoelectric Field-Effect Transistors

Field-effect transistors (FETs) based on nanowires or nanotubes are one of the most-studied nanodevices. A typical NW FET is composed of a semiconducting NW that is connected by two electrodes at its ends and is placed on a silicon substrate covered by a thin layer of gate oxide. A third electrode is built between the NW and the gate oxide (Fig. 10a). The gate voltage (V_G) can trap and deplete the carriers in the NW, thus, controlling the gate voltage can effectively gate the flow of the current from the source to drain electrodes. An NW-based sensor is a source–drain structured NW FET without a gate, thus, a large portion of the NW is exposed to the environment. The mechanism of NW sensors for sensing gases, biomolecules, or even viruses relies on the creation of a charge depletion zone in the semiconductor NW by the surface-adsorbed sensing targets.[34]

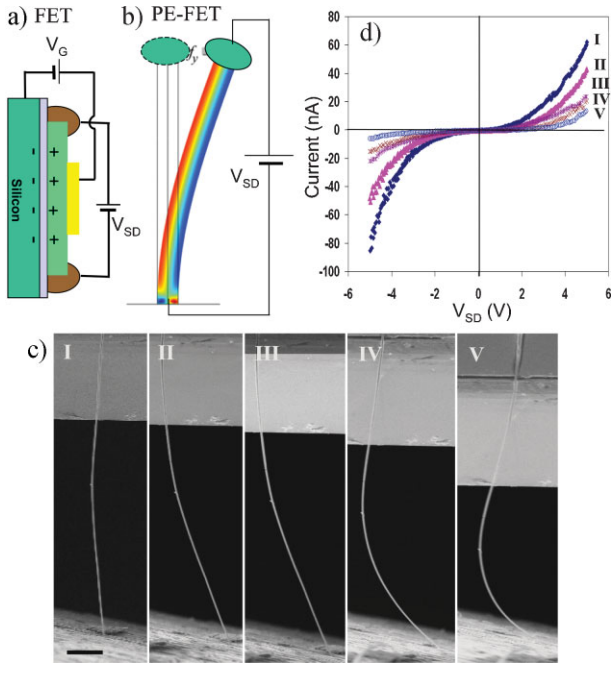

Figure 10. The physical principle of the piezoelectric FET. a) Schematic of a conventional FET that uses a single nanowire/nanobelt, with gate, source, and drain (subscripts G, S, and D, respectively). b) The principle of the piezoelectric FET [32], in which the piezoelectric potential across the nanowire created by the bending force f_y replaces the gate of a conventional FET. The contacts at both ends are ohmic. c) SEM images, each at the same magnification, showing the five typical consecutive bending cases of a ZnO NW; the scale bar represents 10 μm. d) Corresponding *I–V* characteristics of the ZnO nanowire for the five different bending cases.

From the calculation shown in Figure 2, a piezoelectric potential is created across the NW when it is deflected by an external force. If the potential is large enough, it can play the role of V_G for the FET. By connecting a ZnO NW across two electrodes that can apply a bending force to the NW, the electric field created by piezoelectricity across the bent NW serves as the gate for controlling the electric current flowing through the NW (Fig. 10b).[35] Once deformed by an external force, a piezoelectric potential is built across the bent NW, some free electrons in the n-type ZnO NW may be trapped at the positive surface and become non-mobile charges, thus, lowering the effective carrier density in the NW. It is important to note that the trapped ''free charges'' cannot deplete the charges produced by the piezoelectric effect, which are rigid, ionic, and affixed to the atoms. On the other hand, even the positive potential side could be partially screened by the trapped electrons, the negative potential side remains unchanged. The free electrons will be repulsed away by the negative potential and leave a charge depletion zone around the compressed-surface side. Consequently, the width of the conducting channel in the ZnO NW becomes smaller and smaller while the depletion region becomes larger and larger with an increase of the NW bending. The resultant effect is a drastic decrease in conductivity of the NW. This is the proposed piezoelectric FET (PE-FET).

The experimental demonstration of the PE-FET is shown in Figure 10c. A large ZnO wire was in contact with two electrodes. Its transport property was characterized as the wire was bent. Figure 10d shows the corresponding *I–V* curves measured when the wire was bent into shapes shown in Figure 10c, parts I–V. It is clear that the conductance of the NW was reduced by more than ten times after bending. Such an effect was attributed to the gating effect of the piezoelectric potential.

5.2. Piezoelectric Diode

A piezoelectric-field gated diode was demonstrated by using a two-probe technique.[36] One probe held one end of an NW that lay on an insulator substrate, the other probe pushed the NW from the other end by being in contact with the tensile surface. The W tips had ohmic contact with the NW. The *I–V* curve changed from a linear shape to rectifying behavior with an increase in the degree of NW bending (Fig. 11a). This is the piezoelectric diode (PE diode).

The rectifying/switching behavior of the PE diode can be explained from the band diagram shown in Figure 11. Applying an external voltage of V_o between the tip (T) and the root (R) of the NW creates a difference in Fermi levels (E_F) between the tip and the root electrodes, with the root being positive (Fig. 11b). When the tip pushes the NW from the tensile side, a positive V^+ and negative voltage V^- are generated at the tensile and compressive surfaces, respectively, thus, the energy

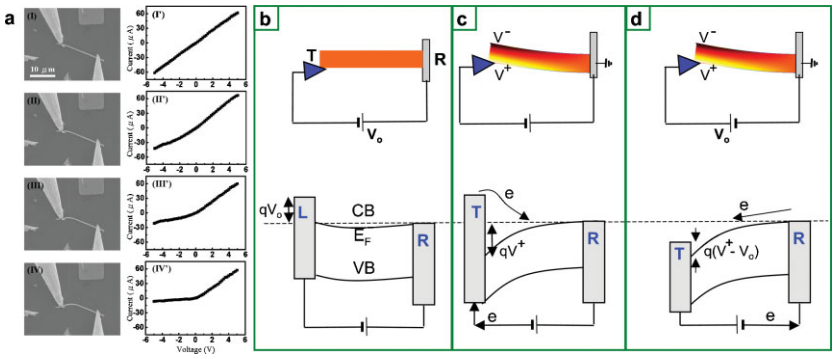

Figure 11. The principle of the piezoelectric field diode, in which one end of an NW is fixed and enclosed by a metal electrode, and the other end is bent by a moving metal tip. Both ends have ohmic contact with ZnO. a) A sequence of SEM images of a ZnO wire at various bending angles and the corresponding *I–V* characteristics, with the fixed probe being positive and the moving tip negative [36]. b) Band diagram of an NW that has ohmic contact at the two ends when a constant voltage V_o is applied, with the tip (T) as negative and root (R) positive. The Fermi level of the tip is raised by qV_o (q is electronic charge). c) Forward bias case: Once the NW is pushed by the tip, a local positive piezoelectric potential at the tensile surface lowers the CB next to the tip, resulting in a forward flow of electrons from the tip through the NW to the root. d) Reverse biased case: When the applied voltage is switched in polarity, the Fermi level of the tip is lowered by qV_o. A potential barrier of height $q(V^+ - V_o)$ is created. Once the applied voltage $V_o < V^+$, the electrons have to transit over the barrier to reach the tip.

level of the conduction band (CB) of the NW next to the tip was lowered by qV^+, with q being the unit charge of the electron (Fig. 11c). In such a case, electrons can easily flow from the tip side to the root side without experiencing any barrier, thus, the transport preserves ohmic behavior. This is the ''forward'' bias of the PE diode.

By switching the polarity of the applied voltage so that the tip has a higher voltage, the Fermi level of the tip is lowed by qV_o in reference to that of the root electrode. Correspondingly, for a case $V_o < V^+$, a barrier of height $q(V^+ - V_o)$ was created for the electrons to flow from the NW to the tip. The transition probability via thermal emission is $\exp[-q(V^+ - V_o)/kT]$. Thus, for $V_o < V^+$, the current decays quickly. This is the ''reversed'' bias of the PE diode. The threshold of the diode increases with increased NW bending.

5.3. Piezoelectric Humidity Sensor

Piezoelectric humidity sensors have been demonstrated by the following experiments.[37] The devices were fabricated using a single ZnO nanobelt (NB) bridging two Au electrodes. Poly(*N*-isopropylacrylamide) (PNIPAM) and poly(diallyldimethylammonium chloride) (PDADMAC) were functionalized alternatively layer-by-layer on the top surface of the NB (Fig. 12a). Measurements on such a conjugated device showed a significant decrease in conductivity upon exposure to 12 and 85% relative humidity (RH) (Fig. 12b). To explore the origin of the reduced current upon vapor exposure, we carried out a series of experiments based on different functional materials on the devices. First, the current response of an uncoated ZnO NB was examined. The result shows a gigantic increase in conductivity (Fig. 12c). Measurement of a conducting channel that contained only multilayers of polymers also showed a drastic increase in conductivity (Fig. 12d), which was in contrast to the response of the polymer-coated NB, as shown in Figure 12b.

The polymers used in our experiments, PNIPAM and PDADMAC, are very sensitive to environmental humidity changes. Upon exposure to water vapor, these polymers undergo a hydration process by absorbing a large amount of H_2O molecules. As a result, the volumes of these polymers increase by a significant amount. Because the polymers were coated only at one side of the ZnO NB, the swelling of the polymers then generated an asymmetric tensile stress at the contact surface with the ZnO NB. Consequently, the ZnO NB was bent into an arc shape under this force, resulting in an asymmetric strain across the thickness of the NB. As shown in Figure 2, a bent ZnO NB could produce a piezoelectric potential across the NB because of the strain-induced piezoelectric effect, which may trap and deplete the carriers in the NB, analogous to the case of the PE-FET, resulting in a decrease of conductivity. This is a different detection mechanism in comparison to the sensors based on FETs.

5.4. Piezoelectric Potential: How Long Does It Last?

For an insulating piezoelectric material, the piezoelectric potential is preserved as long as the strain is maintained. For a

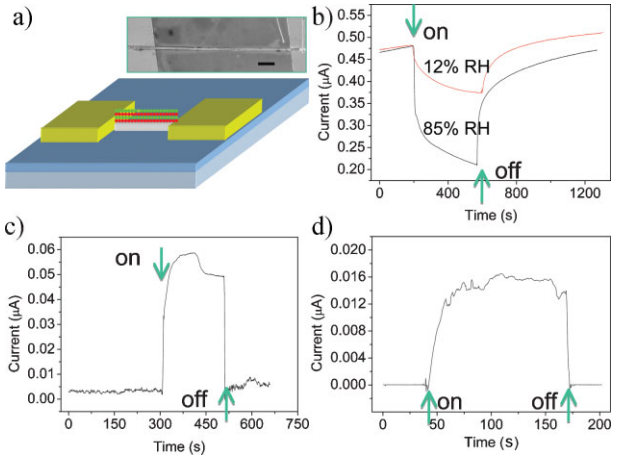

Figure 12. a) Schematic illustration of multilayer deposits of different polymers (red and green) onto the surface of a ZnO NB surface by electrostatic attraction of the charges on the polymers, and an SEM image of such a polymer-functionalized device (Scale bar represents ■). b) Responses of PNIPAM-functionalized devices upon exposure to 12 and 85% relative humidity (RH). c) Current response of an uncoated ZnO NB upon exposure to 85% RH. d) Current response of multilayered polymers in 85% RH vapor [37].

ADVANCED FUNCTIONAL MATERIALS

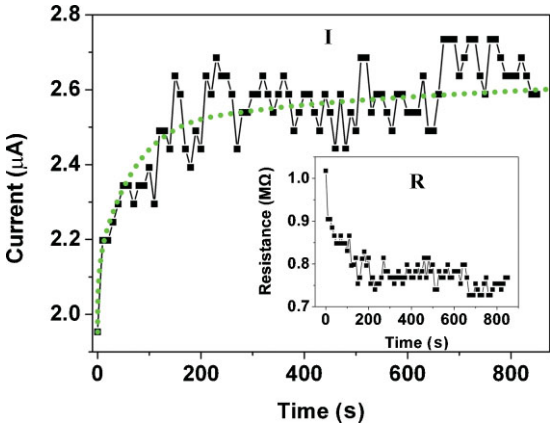

Figure 13. Measuring the effective "lifetime" of the piezoelectric potential created in a ZnO wire after straining. For a fixed bias of 2 V, the current flowing through the bent wire was measured as a function of time. The current reached a steady state after approximately 150 s. The inset is an equivalent plot of the resistance–time (*R–t*) plot, corresponding to the *I–t* curve [25].

material like ZnO with the presence of oxygen vacancies and surfaces, it has moderate conductivity. The question is: how long will the piezoelectric potential be preserved after an NW is bent? We have designed an experiment to measure the lifetime of the piezoelectric potential.[25] The piezoelectric potential created in an NW across its width behaves like an electric field distribution across a parallel-plate capacitor (see Fig. 10b). A method to detect the presence and decay of the piezoelectric field as soon as the NW is bent is to continuously monitor the source–drain *I–V* transport properties of the PE-FET as a function of time. This experiment was carried out by continuously applying a sweeping voltage through the NW and measuring its electric current. By plotting the current measured at a fixed bias of 2 V as a function of time (Fig. 13), a clear trend is seen about the recovery of conductance in the current–time (*I–t*) curve. The long lasting recovery of the current possibly indicates that the electronic effect caused by the piezoelectric characteristic of ZnO extends to as long as 100 s, before they reach a steady state. In addition, piezoresistance is a time-independent effect as long as the strain is fixed.

The slow-screening process is likely caused by the strong trapping effect of the electrons by vacancy/impurity/surface states in ZnO, which results in a slow release of the trapped charges, similar to the recovery of photoconductivity after UV-light excitation.[26] It is possible that the piezoelectric potential created in the NW, if sufficiently large (> bandgap), may excite the electrons in the valence bands to the conduction band or the vacancy/surface states, which hold the charges for an extended period of time, resulting in decreased conductivity. Alternatively, one may suggest that the effect caused by piezoelectric charges and potential could hold for an equivalent length of time before being screened by external electrons to reach a steady state. This is relevant to the piezotronic devices we have proposed.

Furthermore, the trapped charges can drop from the vacancy/surface states back to the valence band, possibly resulting in photon emission. This process is proposed as a piezoelectric-induced photon-emission effect.

5.5. Opto-piezotronic Devices

We have investigated the response of a single CdS-NW-based NG to visible-light excitation.[22] White light reduces the height of the Schottky barrier existing at the tip–NW contact, leading to a possible barrier breakthrough and contact-mode change from Schottky to quasi-ohmic. As a result, a positive voltage output was received when the tip contacted the stretched side of the NW. This is different from the result received when there is no light. This study shows the effectiveness of using light to tune the output of the NG. This work demonstrates the triple coupling effect of semiconducting, piezoelectric, and optoelectric properties, which may be useful for designing new opto-piezotronic devices.

6. Nanowires and Nanobelts of ZnO: Why?

The main materials used for our current studies are one-dimensional nanostructures of ZnO, such as nanowires and nanobelts. In practice, wurtzite-structured materials can also show similar effects, such as CdS-based NGs[38] and GaN.[39,40] The nanowire-based energy-harvesting technology offers a few advantages:

i) The NW/NB can be subjected to extremely large elastic deformation (ca. 90° bending) without plastic deformation or fracture.
ii) Due to their small diameter, NWs/NBs are most likely free of dislocations, and thus, expected to have a high resistance to fatigue, possibly extending the lifetime of the device.
iii) NWs/NBs can be bent under an extremely small applied force. This is unique for harvesting energy created by weak mechanical disturbance.
iv) The large surface area offered by NWs/NBs provides a unique opportunity for surface functionalization to improve physical and chemical properties.
v) ZnO NW arrays can be easily grown via chemical synthesis at 80 °C on any shaped substrate made of any material (crystalline or amorphous, hard or soft), it can be easily integrated with technologically important materials, such as silicon or polymers, at low cost.
vi) ZnO is a biocompatible, degradable, and nontoxic material[41] with a wide range of applications in medicine and cosmetics; thus, it has the most profound potential for implantable and flexible power sources.
vii) ZnO is an environmentally "green" material.

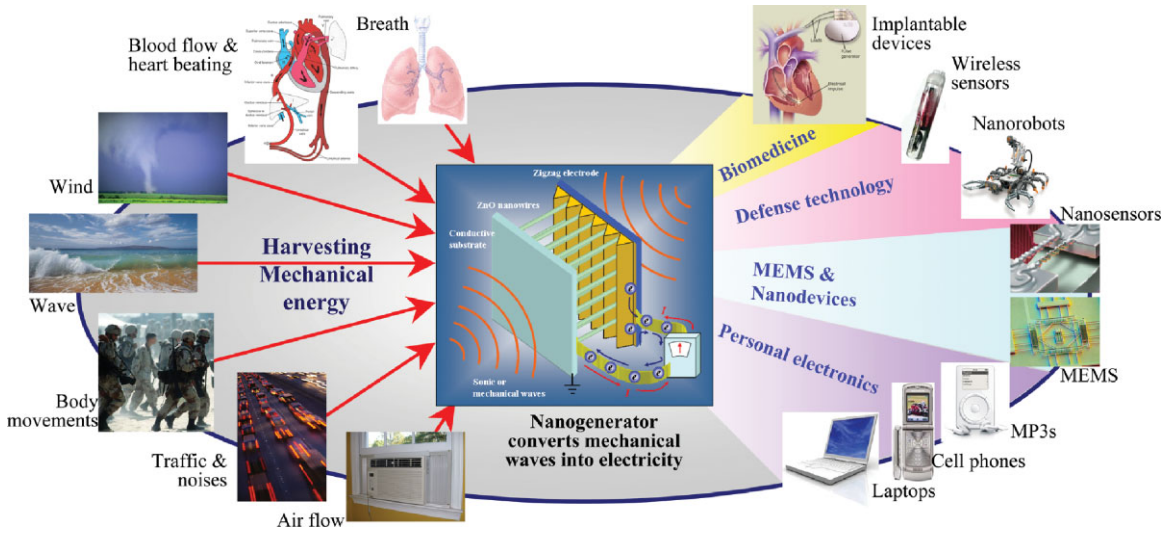

Figure 14. Perspectives of nanogenerators for harvesting mechanical energy and potential future applications.

7. Summary and Perspectives

Future nanotechnology research is likely to focus on the areas of integrating individual nanodevices into a nanosystem that acts like a living species, with sensing, communicating, controlling, and responding abilities. A nanosystem requires a nanometer-scaled power source to make the entire package extremely small and function with high performance. The goal is to make a self-powered nanosystem that can operate wirelessly, independently, and sustainably. Harvesting energy from the environment is a choice for powering nanosystems.

We have systematically reviewed the principle and design of piezoelectric NGs based on aligned ZnO nanowire arrays, which have the potential of converting mechanical energy (such as body movement, muscle stretching, blood pressure), vibrational energy (such as acoustic/ultrasonic waves), and hydraulic energy (such as flow of body fluids, blood flow, contraction of blood vessels, dynamic fluid in nature) into electrical energy that may be sufficient for self-powering nanodevices and nanosystems ranging from biomedical sensors, nanorobots, micro-electromechanical systems (MEMS), and even small personal electronics (Fig. 14). A new period of research into NGs is likely to focus on the following areas:

i) Increasing the number of active NWs for participating electricity generation with the aim of raising the magnitude of the output voltage and power. One approach is to utilize ZnO NW arrays with uniform size, especially uniform length. The other approach is to pattern the NW arrays according to the dimension and shape of the top electrode.
ii) Systematic modeling of the charge generation and transport processes, while comprehensively considering the dynamics involved in mechanics, piezoelectricity, semiconductor physics, and interface contacting.
iii) Developing an effective theory for characterizing the performance of the NG and its efficiency.
iv) Optimizing the dimensionality and design of the NG to obtain the highest energy conversion efficiency.
v) Improving the packaging technology for integrating the electrode and nanowire arrays to achieve the best output.
vi) Study of the failure mechanism of the NG.
vii) Study of the metal–NW interface to build a robust, low-wearing structure for improving the lifetime of the NG.
viii) 3D integration of multiple NGs in order to raise the output voltage and power.
ix) Developing technology for storing the generated charges and raising the voltage by use of available electronics.
x) Integrating NGs with nanodevices towards self-powered nanosystems.

The nano-piezotronics introduced here is a new area of electronics. It utilizes a piezoelectric-field-controlled transport property for achieving unique and new electronic components, such as PE-FETs and PE diodes. Based on the coupled piezoelectric–semiconducting properties, novel electronic devices can be fabricated that are sensitive and controlled by an externally applied force, such as pressure. A near-future research focus will be on building arrays of such devices for applications in areas such as sensors, actuators, triggers, switches, and MEMS.

Received: April 24, 2008
Published online: November 4, 2008

ADVANCED FUNCTIONAL MATERIALS

Note added in proof: Recently, using the strain induced change in transport property of ZnO wire, we have demonstrated a piezoelectric diode based switches with an on-to-off ratio ~120. The wire was laterally bonded and fully packaged, and the design can be easily extended for nanowires, which are expected to have super-high sensitivity. Our studies provide solid evidence about the existence of piezoelectric potential in the ZnO wire although it has a moderate conductivity. The existence of the piezoelectric potential not only supports the mechanism proposed for nanogenerators and piezotronics, but also can be used to fabricate a new type of piezoelectric diodes and switches, which are highly-sensitive, cost-effective, versatile and fully packaged for a wide range of applications.

[1] Special Issue on Sustainability and Energy, *Science* **2007**, *315*, 721.
[2] Special Issue on Harnessing Materials for Energy, *MRS Bull.* **2008**, *33*, No. 4.
[3] Z. L. Wang, *Sci. Am.* **2008**, January, 82.
[4] For a review see J. A. Paradiso, T. Starner, *IEEE Pervasive Comput.* **2005**, *4*, 18.
[5] For a review see E. S. Leland, J. Baker, E. Carleton, E. Reilly, E. Lai, B. Otis, J. M. Rabaey, P. K. Wright, V. Sundararajan, *IEEE Pervasive Comput.* **2005**, *14*, 28.
[6] X. Zheng, T. J. Kempa, Y. Fang, N. Yu, G. Yu, J. Huang, C. M. Lieber, *Nature* **2007**, *449*, 885.
[7] Z. L. Wang, J. H. Song, *Science* **2006**, *312*, 242.
[8] X. D. Wang, J. H. Song, J. Liu, Z. L. Wang, *Science* **2007**, *316*, 102.
[9] Y. Qin, X. D. Wang, Z. L. Wang, *Nature* **2008**, *451*, 809.
[10] Z. L. Wang, *MRS Bull.* **2007**, *32*, 109.
[11] Z. L. Wang, X. Y. Kong, Y. Ding, P. X. Gao, W. L. Hughes, R. S. Yang, Y. Zhang, *Adv. Funct. Mater.* **2004**, *14*, 944.
[12] Z. W. Pan, Z. R. Dai, Z. L. Wang, *Science* **2001**, *209*, 1947.
[13] X. Y. Kong, Z. L. Wang, *Nano Lett.* **2003**, *3*, 1625.
[14] X. Y. Kong, Y. Ding, R. S. Yang, Z. L. Wang, *Science* **2004**, *303*, 1348.
[15] P. X. Gao, Y. Ding, W. J. Mai, W. L. Hughes, C. S. Lao, Z. L. Wang, *Science* **2005**, *309*, 1700.
[16] M. H. Zhao, Z. L. Wang, S. X. X. Mao, *Nano Lett.* **2004**, *4*, 587.
[17] X. D. Wang, J. H. Song, P. Li, J. H. Ryou, R. D. Dupuis, C. J. Summers, Z. L. Wang, *J. Am. Chem. Soc.* **2005**, *127*, 7920.
[18] Z. L. Wang, *J. Nanosci. Nanotechnol.* **2008**, *8*, 27.
[19] X. D. Wang, J. H. Song, Z. L. Wang, *J. Mater. Chem.* **2007**, *17*, 711.
[20] J. H. Song, J. Zhou, Z. L. Wang, *Nano Letters*, **2006**, *6*, 1656.
[21] P. X. Gao, J. H. Song, J. Liu, Z. L. Wang, *Adv. Mater.* **2007**, *19*, 67.
[22] Y.-F. Lin, J. H. Song, Y. Ding, S.-Y. Lu, Z. L. Wang, *Adv. Mater.* **2008**, *20*, 3127.
[23] J. H. Song, X. D. Wang, J. Liu, H. B. Liu, Y. L. Li, Z. L. Wang, *Nano Lett.* **2008**, *8*, 203.
[24] Y. F. Gao, Z. L. Wang, *Nano Lett.* **2007**, *7* 24 995.
[25] J. Zhou, P. Fei, Y. F. Gao, Y. D. Gu, J. Liu, G. Bao, Z. L. Wang, *Nano Lett.*, in press.
[26] J. Liu, P. Fei, J. Zhou, R. Tummala, Z. L. Wang, *Appl. Phys. Lett.* **2008**, *92*, 173 105.
[27] Y. F. Gao, Z. L. Wang, unpublished.
[28] J. Liu, P. Fei, J. H. Song, X. D. Wang, C. S. Lao, R. Tummala, Z. L. Wang, *Nano Lett.* **2008**, *8*, 328.
[29] X. D. Wang, J. Liu, J. H. Song, Z. L. Wang, *Nano Lett.* **2007**, *7*, 2475.
[30] P. X. Gao, J. H. Song, J. Liu, Z. L. Wang, *Adv. Mater.* **2006**, *19*, 67.
[31] *Chem. Eng. News* **2007**, 85.
[32] Z. L. Wang, *Adv. Mater.* **2007**, *19*, 889.
[33] Z. L. Wang, *Mater. Today* **2007**, *10* (No. 5), 20.
[34] G. F. Zheng, F. Patolsky, Y. Cui, W. U. Wang, C. M. Lieber, *Nat. Biotechnol.* **2005**, *23*, 1294.
[35] X. D. Wang, J. Zhou, J. H. Song, J. Liu, N. S. Xu, Z. L. Wang, *Nano Lett.* **2006**, *6*, 2768.
[36] J. H. He, C. H. Hsin, L. J. Chen, Z. L. Wang, *Adv. Mater.* **2007**, *19*, 781.
[37] C. S. Lao, Q. Kuang, Z. L. Wang, M.-C. Park, Y. L. Deng, *Appl. Phys. Lett.* **2007**, *90*, 262 107.
[38] Y.-F. Lin, J. H. Song, Y. Ding, Z. L. Wang, S.-Y. Lu, *Appl. Phys. Lett.* **2008**, *92*, 022 105.
[39] W. S. Su, Y. F. Chen, C. L. Hsiao, L. W. Tu, *Appl. Phys. Lett.* **2007**, *90*, 179 901.
[40] W. S. Su, Y. F. Chen, C. L. Hsiao, L. W. Tu, *Appl. Phys. Lett.* **2007**, *90*, 063 110.
[41] J. Zhou, N. S. Xu, Z. L. Wang, *Adv. Mater.* **2006**, *18*, 2432.